

University of Wollongong

Research Online

---

Australian Institute for Innovative Materials -  
Papers

Australian Institute for Innovative Materials

---

1-1-2013

## Nitrogen removal from natural gas using solid boron: A first-principles computational study

Qiao Sun

*University Of Queensland*

Meng Wang

*China University of Petroleum*

Zhen Li

*University of Wollongong, zhenl@uow.edu.au*

Ping Li

*East China University of Science and Technology*

Weihua Wang

*Qufu Normal University*

*See next page for additional authors*

Follow this and additional works at: <https://ro.uow.edu.au/aiimpapers>



Part of the [Engineering Commons](#), and the [Physical Sciences and Mathematics Commons](#)

---

Research Online is the open access institutional repository for the University of Wollongong. For further information contact the UOW Library: [research-pubs@uow.edu.au](mailto:research-pubs@uow.edu.au)

---

# Nitrogen removal from natural gas using solid boron: A first-principles computational study

## Abstract

Selective separation of nitrogen (N<sub>2</sub>) from methane (CH<sub>4</sub>) is highly significant in natural gas purification, and it is very challenging to achieve this because of their nearly identical size (the molecular diameters of N<sub>2</sub> and CH<sub>4</sub> are 3.64 Å and 3.80 Å, respectively). Here we theoretically study the adsorption of N<sub>2</sub> and CH<sub>4</sub> on B<sub>12</sub> cluster and solid boron surfaces a-B<sub>12</sub> and c-B<sub>28</sub>. Our results show that these electron-deficiency boron materials have higher selectivity in adsorbing and capturing N<sub>2</sub> than CH<sub>4</sub>, which provides very useful information for experimentally exploiting boron materials for natural gas purification.

## Keywords

natural, gas, solid, nitrogen, boron, removal, first, principles, computational, study

## Disciplines

Engineering | Physical Sciences and Mathematics

## Publication Details

Sun, Q., Wang, M., Li, Z., Li, P., Wang, W., Tan, X. & Du, A. (2013). Nitrogen removal from natural gas using solid boron: A first-principles computational study. *Fuel*, 109 (2013), 575-581.

## Authors

Qiao Sun, Meng Wang, Zhen Li, Ping Li, Weihua Wang, Xiaojun Tan, and Aijun Du

# **Nitrogen Removal from Natural Gas using Solid Boron: A First-Principles Computational Study**

Qiao Sun<sup>1\*</sup>, Meng Wang<sup>2</sup>, Zhen Li<sup>3,\*</sup>, Ping Li<sup>4</sup>, Weihua Wang<sup>4</sup>, Xiaojun Tan<sup>5</sup>, and Aijun Du<sup>6\*</sup>

<sup>1</sup> *Centre for Computational Molecular Science, Australian Institute for Bioengineering and Nanotechnology, The University of Queensland, Qld 4072, Brisbane, Australia.*

<sup>2</sup> *Center for Bioengineering and Biotechnology, China University of Petroleum (East China), Qingdao 266555, China.*

<sup>3</sup> *Institute of Superconducting & Electronic Materials, The University of Wollongong, NSW 2500, Australia.*

<sup>4</sup> *School of Chemistry and Chemical Engineering, Qufu Normal University, Qufu, Shandong, 273165, China*

<sup>5</sup> *College of Medical and Life Science, University of Jinan, Jinan, Shandong, 250022, China.*

<sup>6</sup> *School of Chemistry, Physics and Mechanical Engineering, Queensland University of Technology, Brisbane, QLD 4001, Australia*

---

Corresponding author: Qiao Sun, Zhen Li and Aijun Du

Email: q.sun@uq.edu.au; zhenl@uow.edu.au; aijun.du@qut.edu.au

## **Abstract**

Selective separation of nitrogen ( $N_2$ ) from methane ( $CH_4$ ) is highly significant in natural gas purification, and it is very challenging to achieve this because of their nearly identical size (the molecular diameters of  $N_2$  and  $CH_4$  are 3.64 Å and 3.80 Å, respectively). Here we theoretically study the adsorption of  $N_2$  and  $CH_4$  on  $B_{12}$  cluster and solid boron surfaces  $\alpha$ - $B_{12}$  and  $\gamma$ - $B_{28}$ . Our results show that these electron-deficiency boron materials have higher selectivity in adsorbing and capturing  $N_2$  than  $CH_4$ , which provides very useful information for experimentally exploiting boron materials for natural gas purification.

**Keywords**  $N_2/CH_4$  separation; Gas purification; DFT calculations

## **Introduction**

The demand for natural gas is expected to increase continuously in the coming years, because natural gas produces lower  $CO_2$  emission than other fossil fuels. Novel transport technologies, the remarkable reserves found, the lower overall costs and the environmental sustainability all point to natural gas as the primary energy source in the near future.[1, 2] In fact, the demand for natural gas may exceed coal by 2020, due to its less pollution and higher use efficiency.[3] The natural gas reservoirs are usually far from final markets, and as a consequence it has to be transported either by pipelines as a gaseous mixture containing at least 75% of methane, or by tankers as liquified natural gas containing at least 85% of methane.[4] The choice between the two transportation technologies depends mainly on the distance and the volume of gas to be transferred.

Nitrogen is a common contaminant in natural gas and is quite difficult to be removed. It lowers the value of the natural gas and makes it untransportable to most pipelines. Natural gas can be accepted for pipeline transport -only it contains less amount of nitrogen, typically between 4% and 6%. Therefore several approaches (e.g. cryogenic separation, solid adsorption and membrane separation) have been developed for removing nitrogen. Cryogenic nitrogen removal is complex and expensive, prohibiting large-scale purification of natural gas.[5] Solid adsorption has been proposed as attractive alternatives for natural gas purification. However, most sorbents show weak interactions with methane and nitrogen, and unable to effectively separate them.[3] Conventional membrane technology cannot effectively separate nitrogen from natural gas because of the similar molecules kinetic diameters of methane and nitrogen ( $\sigma_{N_2} = 3.64 \text{ \AA}$ ,  $\sigma_{CH_4} = 3.80 \text{ \AA}$ ).[6] Thus, very few materials are able to selectively adsorb nitrogen from natural gas, and it is highly significant to seek new materials with high selectivity and low cost for separation of nitrogen from natural gas.

In recent years, novel boron clusters and boron crystals have attracted extensive attentions,[7-15] due to their unique physicochemical properties.[12, 16-19] There are growing interests in exploring the structures and properties of pure boron clusters and boron containing compounds because they have a wide variety of applications from nuclear reactors to superhard, thermoelectric and high energy materials. In the recent article "Boron Cluster Come of Age", Grimes commented the variety of boron clusters, such as neutral boranes, polyhedral boranes, and their derivatives, motivating us to reconsider the concept of covalent chemical bonding.[20] Among boron clusters,  $B_{12}$  icosahedron is the basic structural unit for the elementary boron solids (e.g. the well-known  $\alpha$ - $B_{12}$  and  $\gamma$ - $B_{28}$  crystals) although the  $B_{12}$  icosahedron is not stable when it is treated as a single isolated cluster.[21-24] Recently, boron-rich ternary compounds

containing  $B_{12}$  icosahedra have attracted considerable attention since they exhibit important features on both fundamental and practical perspectives.[7, 9, 12, 25-27]

For crystal boron, the central unit (i.e.  $B_{12}$  icosahedron) of their structures is same to that of many boron rich compounds, and can be flexibly linked, joined, or fused into rigid framework structures.[12, 16-18, 21, 25, 26, 28-31] The formation of  $B_{12}$  unit and its versatile connectivity are attributed to the “electron deficiency”, or hypovalency of boron. There are only four crystal phases reported for pure elementary boron: rhombohedral  $\alpha$ - $B_{12}$ [17, 26, 31] and  $\beta$ - $B_{106}$ [16](with 12 and 106 atoms in the unit cell, respectively), tetragonal T-192[18] (with 190–192 atoms per unit cell) and  $\gamma$ - $B_{28}$  (with 28 atoms in the unit cell).  $\alpha$ - $B_{12}$  consists of one  $B_{12}$  icosahedron per unit cell while  $\gamma$ - $B_{28}$  consists of icosahedral  $B_{12}$  clusters and  $B_2$  pairs in a NaCl-type arrangement.[12] Moreover, the electronic properties of the  $B_2$  pairs and  $B_{12}$  clusters in  $\gamma$ - $B_{28}$  are different, resulting in the charge transfer between  $B_{12}$  clusters and  $B_2$  pairs.[12] In this paper, we investigate the adsorption of  $N_2$  and  $CH_4$  on boron  $B_{12}$  icosahedron cluster and boron solid surfaces of  $\alpha$ - $B_{12}$  and  $\gamma$ - $B_{28}$ . The primary motivation is to identify solid boron crystals as new sorbents for natural gas purification.

### **Computational methods**

The first-principles density-functional theory [32, 33] with long range dispersion correction[34] (DFT-D) calculations were carried out using DMol3 module in Materials Studio.[35, 36] The boron cluster and boron solid surfaces were fully optimized in the given symmetry using generalized gradient approximation treated by Perdew-Burke-Ernzerhof exchange-correlation potential. An all electron double numerical atomic orbital augmented by  $d$ -polarization functions (DNP) was used as basis set. The self-consistent field (SCF) procedure was used with a

convergence threshold of  $10^{-6}$  a.u. on energy and electron density. The direct inversion of the iterative subspace technique developed by Pulay was used with a subspace size 6 to speed up SCF convergence on these large clusters.[37] In order to achieve the SCF convergence when the gap between the highest occupied molecular orbital and the lowest unoccupied molecular orbital (HOMO-LUMO) is small, thermal smearing using finite-temperature Fermi function of 0.005 a.u. was used. Geometry optimizations were performed with a convergence threshold of 0.002 a.u./Å on the gradient, 0.005 Å on displacements, and  $10^{-5}$  a.u. on the energy. The real-space global cutoff radius was set to be 4.10 Å. For the B<sub>12</sub> cluster, the cluster was placed in a sufficiently large supercell (20 Å × 20 Å × 20 Å) to avoid interactions with its periodic images. The cell parameters for α-B<sub>12</sub> and γ-B<sub>28</sub> used for the calculations are all optimized. The optimized cell parameters of α-B<sub>12</sub> and γ-B<sub>28</sub> are in good agreement with experimental measurements. In details, the optimized cell parameters of α-B<sub>12</sub> are with the values of a=b=c=5.052 Å, α=β=γ=57.76°, which are very close to the values of experimental measurement of a=b=c=5.064 Å, α=β=γ=58.10 °.[38] For γ-B<sub>28</sub>, the optimized cell parameters are a=5.042 Å, b=5.598 Å, c=6.914 Å, α=β=γ=90.0 °, which are also consistent with the experimental values of a=5.054 Å, b=5.612 Å, c=6.987 Å, α=β=γ=90.0 °.[12] The 4 × 4 α-boron (001) and 2 × 2 γ-boron (001) surfaces were chosen with 15 Å vacuum in order to avoid interactions with its periodic images, and the slab thicknesses of α-B<sub>12</sub> and γ-B<sub>28</sub> are 8.012 Å and 6.914 Å, respectively. The fully relaxed α-B<sub>12</sub> (001) surface with cell vectors is shown in Figure 1. **Here we need to point out that the (001) surface of the current study is in a rhombohedral setting and the (001) surfaces of earlier studies [26, 31, 38] are in hexagonal settings.** The Brillouin zone was sampled by 6 × 6 × 1 k-points using the Monkhorst-Pack scheme. The calculations of N<sub>2</sub> and CH<sub>4</sub> adsorption on α-B<sub>12</sub> (001) and γ-B<sub>28</sub> (001) surfaces are based on the fully optimized surfaces. We have considered all the

possible adsorption sites for N<sub>2</sub> and CH<sub>4</sub> adsorption on  $\alpha$ -B<sub>12</sub> and  $\gamma$ -B<sub>28</sub> surfaces. What we discussed in the manuscript is the most stable adsorption site. The transition state between chemisorption and physisorption of N<sub>2</sub> was investigated using the complete LST (linear synchronous transit)/QST (quadratic synchronous transit) method [39] implemented in Dmol3 code.

The adsorption energy of N<sub>2</sub> and CH<sub>4</sub> on B<sub>12</sub> cluster,  $\alpha$ -B<sub>12</sub> and  $\gamma$ -B<sub>28</sub> surfaces are calculated from Eq. 1.

$$E_{ads} = (E_B + E_{gas}) - E_{B-gas} \quad (1)$$

where  $E_{B-gas}$  is the total energy of boron adsorbent with adsorbed gas,  $E_B$  is the energy of isolated boron adsorbent, and  $E_{gas}$  is the energy of isolated gas molecule, such as N<sub>2</sub> and CH<sub>4</sub>. Electron distribution and transfer mechanism are conducted by Mulliken method.[40]

To better clarify the adsorption and the nature of the interaction of N<sub>2</sub> and CH<sub>4</sub> on B<sub>12</sub> cluster,  $\alpha$ -B<sub>12</sub> and  $\gamma$ -B<sub>28</sub> surfaces, the atoms in molecules (AIM) theory which has been used to successfully determine intermolecular interactions of different systems has been employed using wavefunctions at B3LYP/6-311+G(d) level of theory.[41-47] The configurations for AIM calculations are based on the optimized structures at DFT-D level. In the AIM analyses, the existence of the interaction is indicated by the presence of a so-called bond critical point (BCP). The strength of the bond can be estimated from the magnitude of the electron density ( $\rho_{bcp}$ ) at the BCP. Similarly, the ring or cage structures are characterized by the existence of a ring critical point (RCP) or cage critical point (CCP). Furthermore, the nature of the molecular interaction can be predicted from the topological parameters at the BCP, such as the Laplacian of electron density ( $\nabla^2\rho_{bcp}$ ) and energy density ( $H_{bcp}$ ). Generally, the sign of  $\nabla^2\rho_{bcp}$  reveals whether charge is concentrated ( $\nabla^2\rho_{bcp} < 0$ ) as in covalent bonds (shared interaction) or depleted ( $\nabla^2\rho_{bcp} > 0$ ) as



in ionic bonds, H-bonds, and van der Waals interactions (closed-shell interaction). The topological analysis of the system was carried out via the AIMALL program.[48]

## **Results and Discussions**

Separation of N<sub>2</sub> from CH<sub>4</sub> is highly significant in natural gas purification. To the best of our knowledge, it is the first time to perform the first-principles DFT-D calculations of N<sub>2</sub> and CH<sub>4</sub> adsorption on B<sub>12</sub> cluster,  $\alpha$ -B<sub>12</sub> and  $\gamma$ -B<sub>28</sub>. Our results demonstrate the adsorption energies of N<sub>2</sub> on these materials are much higher than those of CH<sub>4</sub>, which indicates the boron crystals have high selectivity in capturing N<sub>2</sub> from natural gas.

### **N<sub>2</sub> adsorption on B<sub>12</sub> cluster, $\alpha$ -B<sub>12</sub> and $\gamma$ -B<sub>28</sub>**

In this part, we will discuss the DFT-D calculational results of N<sub>2</sub> adsorption on B<sub>12</sub> icosahedron cluster,  $\alpha$ -B<sub>12</sub> and  $\gamma$ -B<sub>28</sub> surfaces. We will start with the CH<sub>4</sub> adsorption on B<sub>12</sub> cluster. The configurations of N<sub>2</sub> adsorption on B<sub>12</sub> cluster are shown in Figure 2. Correspondingly, the geometrical parameters and the physical and chemical adsorption energies are summarized in Table 1. For free N<sub>2</sub> molecule, the N–N bond length is calculated to be 1.109 Å. In its physisorbed configuration (Figure 2 (a)), N<sub>2</sub> is far from the B<sub>12</sub> cluster with a distance of 2.990 Å. The molecular graphs of those geometries have been given in Figure 3. As displayed in Figure 3(a), the interaction between N<sub>2</sub> and B<sub>12</sub> cluster can be confirmed by the existence of the bond critical point (BCP) of the N<sub>2</sub>–B contact. The corresponding topological parameters at the BCP have been presented in Table S2 in supporting information. Obviously, the electron densities at the BCPs of the N<sub>2</sub>-B between N<sub>2</sub> and B<sub>12</sub> cluster are small (Table S2), which indicates the interaction is very weak and it is mainly come from the van der Waals interactions between N<sub>2</sub> and B<sub>12</sub> cluster. Because of the weak interaction, the physisorbed N<sub>2</sub> molecule (N-N bond length = 1.110 Å) almost did not undergo noticeable structural change compared with the free N<sub>2</sub> (N-N

bond length in gas phase is 1.109 Å). The Mulliken charge distributions of configurations of N<sub>2</sub> adsorption on B<sub>12</sub> cluster and charge transfer between N<sub>2</sub> and B<sub>12</sub> cluster are listed in supporting information Table S1. The charge transfer from N<sub>2</sub> to B<sub>12</sub> cluster is negligible and the value is -0.002 e. The adsorption energy of N<sub>2</sub> molecule on B<sub>12</sub> cluster is calculated to be 0.08 eV. In addition, our study also shows the physisorption process has no transition state.

In its chemisorption configuration (Figure 2 (c)), the distance between one boron atom in B<sub>12</sub> cluster and one nitrogen atom in N<sub>2</sub> molecule is 1.515 Å. The adsorption energy is calculated to be 0.38 eV on PAW-PBE level, which suggests the chemisorption is a thermally favourable process. In the chemisorption, triple-bond of N<sub>2</sub> molecule is broken and slightly elongated to 1.132 Å on top of the B, compared with that of N<sub>2</sub> molecule in gas phase (with N-N bond length of 1.109 Å). The B-B bond connecting with N<sub>2</sub> is also considerably pulled out and elongated by 0.05 Å. Once the chemisorption is formed, there is 0.113 negative charge spontaneously transferring from N<sub>2</sub> molecules to B<sub>12</sub> cluster because of “electron deficiency” of B<sub>12</sub> cluster.

We performed LST/QST calculation to identify the transition state between physisorption and chemisorption configurations. As shown in Table S2, the electron densities at the BCPs for the N<sub>2</sub>-B bonds of physisorption (Figure 2(a)), transition state (Figure 2(b)), and chemisorptions (Figure 2(c)) increased gradually, which is consistently with the adsorption process from weak to strong interaction as well as the bond distances decrease from the values of 2.990 Å to 2.287 Å and 1.515 Å for the three structures, respectively. The imaginary frequency of the transition state is 130.4i cm<sup>-1</sup> and it is assigned to the stretch mode of NN-B bond for formation of chemisorption configuration from its physisorption analogue. The results show the reactants need to overcome a barrier of 0.04 eV from the reaction path of its physisorption to chemisorption.

The very low energy barrier for the reaction of N<sub>2</sub> adsorption from physisorption to chemisorption indicates that it is a kinetically favourable process.

In order to explore the application of boron crystals for natural gas separation, we also performed the DFT-D calculations of N<sub>2</sub> adsorption on  $\alpha$ -B<sub>12</sub> (001) and  $\gamma$ -B<sub>28</sub> (001) surfaces. The configurations of N<sub>2</sub> adsorption on  $\alpha$ -B<sub>12</sub> and  $\gamma$ -B<sub>28</sub> are shown in Figure 2. Their important geometrical parameters and adsorption energies are also summarized in Table 1. In contrast to the adsorption of N<sub>2</sub> on B<sub>12</sub> cluster, we only gained chemisorption configurations for  $\alpha$ -B<sub>12</sub> and  $\gamma$ -B<sub>28</sub> surfaces, in which N<sub>2</sub> molecules are tightly bound to the surface of  $\alpha$ -B<sub>12</sub> and  $\gamma$ -B<sub>28</sub> with adsorption energies of 1.20 eV and 1.07 eV, respectively. In their configurations, the triple-bonds of N<sub>2</sub> molecules are broken and N-N bonds are slightly elongated to 1.126 Å and 1.124 Å on top of the B of  $\alpha$ -B<sub>12</sub> and  $\gamma$ -B<sub>28</sub> surfaces, respectively. The B-B bonds connected with N<sub>2</sub> are also considerably elongated around 0.06 ~ 0.13 Å of the two surfaces. The distances between B atom and N atom are 1.469 Å and 1.479 Å for  $\alpha$ -B<sub>12</sub> and  $\gamma$ -B<sub>28</sub>, respectively, which are shorter than that of N<sub>2</sub> adsorption on B<sub>12</sub> cluster. This indicates the stronger interactions of N<sub>2</sub> with  $\alpha$ -B<sub>12</sub> and  $\gamma$ -B<sub>28</sub>, which can be supported by the relatively larger electron densities at the BCPs for the N<sub>2</sub>-B bond of the two configurations. Once the chemisorptions are formed, there are 0.141 negative charges spontaneously transferring from N<sub>2</sub> to  $\alpha$ -B<sub>12</sub> and  $\gamma$ -B<sub>28</sub> because of “electron deficiency” of the boron solid. Our results demonstrate those chemisorption reactions have no transition state and the reactions are no barrier, and the adsorptions are kinetically favourable. Therefore, N<sub>2</sub> molecules adsorption on  $\alpha$ -B<sub>12</sub> and  $\gamma$ -B<sub>28</sub> surfaces are energetically and kinetically favourable processes. The adsorption of N<sub>2</sub> on  $\alpha$ -B<sub>12</sub> surface is slightly more favorable than that of on  $\gamma$ -B<sub>28</sub> surface. Here we need to mention that McElligott and Roberts’ study showed that N<sub>2</sub> did not chemisorb on boron films of amorphous boron,[49] while our calculational results indicate that

N<sub>2</sub> molecules can form chemical bindings with  $\alpha$ -B<sub>12</sub> and  $\gamma$ -B<sub>28</sub> crystal surfaces. The reason of the adsorption properties of amorphous boron is different from the crystalline forms might be that, in amorphous boron, the boron icosahedra are bonded randomly to each other without long-range order, and there will be more deformations and form more covalent bonds in amorphous boron than that of crystal boron, and the adsorption sites in crystal boron might have more dangling bonds than that of amorphous boron, so the adsorption sites with more dangling bonds in crystal boron could form strong interaction with nitrogen while the amorphous boron cannot.

#### **CH<sub>4</sub> adsorption on B<sub>12</sub> cluster, $\alpha$ -B<sub>12</sub> and $\gamma$ -B<sub>28</sub>**

In order to understand the interaction properties between the boron materials and CH<sub>4</sub> molecules, we also calculated the adsorption of CH<sub>4</sub> on B<sub>12</sub> cluster,  $\alpha$ -B<sub>12</sub> and  $\gamma$ -B<sub>28</sub> surfaces. The calculated C–H bond length and H–C–H angle in free CH<sub>4</sub> molecule are 1.098 Å and 109.4°, respectively. In the following part, we will first discuss the adsorption of CH<sub>4</sub> on B<sub>12</sub> cluster. The important structural parameters of CH<sub>4</sub> adsorption on B<sub>12</sub> cluster are listed in Table 2. From the calculation we can only find CH<sub>4</sub> adsorbed on B<sub>12</sub> cluster by physisorbed configuration. The C...B and H...B distances of CH<sub>4</sub> on the sorbent are 3.557 Å and 2.833 Å, respectively. We can see that the distance between CH<sub>4</sub> and the adsorbent is quite far and the adsorption energy is only 0.08 eV. The charge transfer from CH<sub>4</sub> to B<sub>12</sub> cluster is negligible and with the value of 0.002 e (Table S1). These results indicate their interaction is very weak and it mainly arises from the van der Waals force between CH<sub>4</sub> and B<sub>12</sub> cluster. Because of the weak interaction, the physisorbed CH<sub>4</sub> did not undergo noticeable structural changes compared with the geometry of free CH<sub>4</sub>. The changes in two C-H bonds (1.098 Å) nearby B<sub>12</sub> cluster are negligible compared with those of free CH<sub>4</sub> (1.099 Å). The same situation occurs for H-C-H angle which slightly decreases from

109.5 to 108.9°. As displayed in Figure 3 (d), the interaction between CH<sub>4</sub> and B<sub>12</sub> cluster can be confirmed by the existence of the bond critical point (BCP) of the H–B contact. Obviously, the electron densities at the BCPs of the H-B between CH<sub>4</sub> and B<sub>12</sub> cluster are small (Table S2). Therefore CH<sub>4</sub> can be weakly adsorbed on B<sub>12</sub> cluster, which is contrast to the adsorption of N<sub>2</sub> on B<sub>12</sub> cluster.

The CH<sub>4</sub> adsorption on  $\alpha$ -B<sub>12</sub> and  $\gamma$ -B<sub>28</sub> surfaces is also investigated for comparison. The important structural properties of CH<sub>4</sub> adsorption on  $\alpha$ -B<sub>12</sub> and  $\gamma$ -B<sub>28</sub> are also listed in Table 2. From the calculational results we can see that the distances between CH<sub>4</sub> and  $\alpha$ -B<sub>12</sub>,  $\gamma$ -B<sub>28</sub> sorbents are quite far. The C...B distances of CH<sub>4</sub> on  $\alpha$ -B<sub>12</sub> and  $\gamma$ -B<sub>28</sub> are 3.255 Å and 3.380 Å, respectively, and H...B distances of CH<sub>4</sub> on  $\alpha$ -B<sub>12</sub> and  $\gamma$ -B<sub>28</sub> are 2.807 Å and 2.676 Å, respectively. The charge transfer from CH<sub>4</sub> to  $\alpha$ -B<sub>12</sub> and  $\gamma$ -B<sub>28</sub> are negligible and with the values of 0.006 e and 0.014 e, respectively. CH<sub>4</sub> is adsorbed on the two adsorbents by physical adsorption and the adsorption energies on  $\alpha$ -B<sub>12</sub> and  $\gamma$ -B<sub>28</sub> are 0.17 eV and 0.14 eV, respectively. In addition, we can see from Table S2 that the electron densities at the BCPs of the H-B bonds between CH<sub>4</sub> and the two adsorbents are small, which are consistent with their weak interactions. In comparison with the interactions between N<sub>2</sub> and the two adsorbents, the interactions between CH<sub>4</sub> and  $\alpha$ -B<sub>12</sub> as well as  $\gamma$ -B<sub>28</sub> are very weak. This demonstrates that  $\alpha$ -B<sub>12</sub> and  $\gamma$ -B<sub>28</sub> have higher affinity to N<sub>2</sub> and they can be used to separate N<sub>2</sub> from N<sub>2</sub>/CH<sub>4</sub> mixture.

The difference of adsorption energy among N<sub>2</sub> and CH<sub>4</sub> adsorbed on the three boron compounds can be understood by analysis of the energy-gaps between their highest occupied molecular orbitals (LUMO) and lowest unoccupied molecular orbitals (HOMO). According to the molecular orbital theory, the frontier orbits and nearby molecular orbits are the most important factors determining the stability of the molecule. The larger the difference between the LUMO-

HOMO frontier orbitals, the more stable the molecular structure is. The energy gaps of  $\Delta E$  ( $\Delta E = E_{\text{LUMO}} - E_{\text{HOMO}}$ ) for  $B_{12}$  cluster,  $\alpha\text{-}B_{12}$  and  $\gamma\text{-}B_{28}$  surfaces are 2.103 eV, 0.046 eV and 0.854 eV, respectively. It is clearly observed the energy gaps of the three boron materials are in the order of  $\alpha\text{-}B_{12} < \gamma\text{-}B_{28} < B_{12 \text{ cluster}}$ . The narrower LUMO-HOMO energy-gap means the higher activity of molecule. The energy gaps of the three boron materials can explain the strength of the interactions of  $N_2$  with the three sorbents which are in the order of  $\alpha\text{-}B_{12}$  (adsorption energy 1.20 eV)  $>$   $\gamma\text{-}B_{28}$  (adsorption energy 1.07 eV)  $>$   $B_{12 \text{ cluster}}$  (adsorption energy 0.38 eV). Although the adsorption energies of  $CH_4$  on  $B_{12}$  cluster,  $\alpha\text{-}B_{12}$  and  $\gamma\text{-}B_{28}$  surfaces are in the same order, their values are very small (0.08 ~ 0.17 eV) and the interactions between  $CH_4$  and all boron materials are very weak. The big differences of the adsorption energies of the two gases on the two boron crystals demonstrate that the boron crystals are very good materials for  $N_2/CH_4$  separation. In addition, the selectivity of  $\alpha\text{-}B_{12}$  is higher than that of  $\gamma\text{-}B_{28}$ . Moreover, from our results we can predict that other “electron deficiency” boron solids, such as  $\beta\text{-}B_{106}$  and T-192 could also be used as promising materials for natural gas purification.

## Conclusions

In summary, we have calculated the adsorptions of  $CH_4$  and  $N_2$  on  $B_{12}$  cluster,  $\alpha\text{-}B_{12}$  and  $\gamma\text{-}B_{28}$  surfaces. With all the three materials,  $CH_4$  forms weak interactions with them and the adsorption energies are among 0.08 ~ 0.17 eV. However,  $N_2$  molecules form strong chemical interactions with them and the adsorption energies of  $N_2$  adsorption on  $B_{12}$  cluster,  $\alpha\text{-}B_{12}$  and  $\gamma\text{-}B_{28}$  are 0.37, 1.20 and 1.07 eV, respectively. The results also show the adsorptions of  $N_2$  on these boron sorbents have very low energy barrier or no energy barrier. The study demonstrates that “electron deficiency” boron crystals have high ability of  $N_2$  capture and high selectivity for

N<sub>2</sub>/CH<sub>4</sub> mixture separation. These materials could serve as promising adsorbents for natural gas purification.

## Acknowledgements

We are grateful to the Australian Research Council and China NSFC (21003082) for supporting this work. We also acknowledge generous grants of high performance computer time from both The University of Queensland and the National Computational Infrastructure (NCI).

## Captions

**Figure 1** The fully relaxed  $\alpha$ -B<sub>12</sub> (001) surface with cell vectors and the surface is in a rhombohedral setting. Atom color code: pink, boron.

**Figure 2** (a), (b), (c) and (d) are side and top view of optimized configurations of N<sub>2</sub> and CH<sub>4</sub> adsorption on B<sub>12</sub> cluster. (e), (f), (g) and (h) are side view of the slabs and top view of the surfaces of optimized configurations of N<sub>2</sub> and CH<sub>4</sub> adsorption on  $\alpha$ -B<sub>12</sub> and  $\gamma$ -B<sub>28</sub>. Atom color code: blue, nitrogen; pink, boron; dark gray, carbon; light gray, hydrogen.

**Figure 3** The molecular graphs of the intermediates and transition state of N<sub>2</sub> and CH<sub>4</sub> adsorption on B<sub>12</sub> cluster,  $\alpha$ -B<sub>12</sub> and  $\gamma$ -B<sub>28</sub> surfaces, where the bond critical points (BCPs), ring critical points (RCPs) and cage critical point (CCP) are denoted as small green, red and blue dots, respectively.

**Table 1** Adsorption energy in eV, bond distance ( $r$ ) in Å and bond angle ( $\alpha$ ) in deg for the configurations of N<sub>2</sub> adsorption on B<sub>12</sub> cluster,  $\alpha$ -B<sub>12</sub> and  $\gamma$ -B<sub>28</sub> surfaces.

**Table 2** Adsorption energy in eV, bond distance ( $r$ ) in Å and bond angle ( $\alpha$ ) in deg for the configurations CH<sub>4</sub> adsorption on B<sub>12</sub> cluster,  $\alpha$ -B<sub>12</sub> and  $\gamma$ -B<sub>28</sub> surfaces.

## References

- [1] Eni sustainability report, 2006, [www.eni.it](http://www.eni.it).
- [2] Eni world oil & gas review, 2007, [www.eni.it](http://www.eni.it).
- [3] Tagliabue M, Farrusseng D, Valencia S, Aguado S, Ravon U, Rizzo C, Corma A, Mirodatos C. *Chem. Eng. J.* 2009; 155: 553.
- [4] Kidnay AJ, Parrish WR. *Fundamentals of Natural Gas Processing*, Taylor & Francis, Boca Raton, USA, 2006.
- [5] Daimiger U, Lind W. Adsorption processes for natural gas treatment: a technology update, Engelhard Brochure 2004.
- [6] D.W. Breck. *Zeolite Molecular Sieves*, John Willey & Sons, New York, USA, 1974.
- [7] Häussermann U, Mikhaylushkin AS. *Inorg. Chem.* 2010; 49: 11270.
- [8] Zhao JJ, Wang L, Li FY, Chen ZF. *J. Phys. Chem. A* 2010; 114: 9969.
- [9] Oganov AR, Solozhenko VL. *J. Superhard Mat.* 2009; 31: 285.
- [10] Li M, Li Y, Zhou Z, Shen P, Chen Z. *Nano Lett.* 2009; 9: 1944.
- [11] Zhao YF, Lusk MT, Dillon AC, Heben MJ, Zhang SB. *Nano Lett.* 2008; 8: 157.
- [12] Oganov AR, Chen J, Gatti C, Ma Y, Ma Y, Glass CW, Liu Z, Yu T, Kurakevych OO, Solozhenko VL. *Nature* 2009; 457: 863.
- [13] Bean DE, Muya JT, Fowler PW, Minh Tho N, Ceulemans A. *Phys. Chem. Chem. Phys.* 2011; 13: 20855.
- [14] Wang Y, Robinson GH. *Science* 2011; 333: 530.
- [15] Gonzalez Szwacki N, Sadrzadeh A, Yakobson BI. *Phys. Rev. Lett.* 2007; 98: 166804.
- [16] Sands DE, Hoard JL. *J. Am. Chem. Soc.* 1957; 79: 5582.
- [17] McCarty LV, Kasper JS, Horn FH, Decker BF, Newkirk AE. *J. Am. Chem. Soc.* 1958; 80: 2592.
- [18] Talley CP. *Acta Cryst.* 1960; 13: 271.
- [19] Szwacki NG, Sadrzadeh A, Yakobson BI. *Phys. Rev. Lett.* 2007; 98: 166804.
- [20] Grimes RN. *J. Chem. Educ.* 2004; 81: 658.
- [21] Kawai R, Weare JH. *J. Chem. Phys.* 1991; 95: 1151.
- [22] Boustani I. *Chem. Phys. Lett.* 1995; 240: 135.
- [23] Boustani I. *Phys. Rev. B* 1997; 55: 16426.
- [24] Zhai HJ, Kiran B, Li J, Wang LS. *Nature Mater.* 2003; 2: 827.



- [25] He JL, Wu ED, Wang HT, Liu RP, Tian YJ. *Phys. Rev. Lett.* 2005; 94: 015504.
- [26] Marlid B, Larsson K, Carlsson JO. *J. Phys. Chem. B* 2001; 105: 12797.
- [27] Wagner P, Ewels CP, Suarez-Martinez I, Guiot V, Cox SFJ, Lord JS, Briddon PR. *Phys. Rev. B* 2011; 83: 024101.
- [28] Hubert H, Devouard B, Garvie LAJ, O'Keeffe M, Buseck PR, Petuskey WT, McMillan PF. *Nature* 1998; 391: 376.
- [29] Franz R, Werheit H. *Europhys. Lett.* 1989; 9: 145.
- [30] Li D, Xu YN, Ching WY. *Phys. Rev. B* 1992; 45: 5895.
- [31] Decker BF, Kasper JS. *Acta Cryst.* 1959; 12: 503.
- [32] Zhao Y, Truhlar DG. *J. Chem. Theory Comput.* 2007; 3: 289.
- [33] Thanthiriwatte KS, Hohenstein EG, Burns LA, Sherrill CD. *J. Chem. Theory Comput.* 2011; 7: 88.
- [34] Grimme S. *J. Comput. Chem.* 2006; 27: 1787.
- [35] Delley B. *J. Chem. Phys.* 1990; 92: 508.
- [36] Delley B. *J. Chem. Phys.* 2000; 113: 7756.
- [37] Pulay P. *J. Comput. Chem.* 1982; 3: 556.
- [38] Will G, Kiefer B. *Z. Anorg. Allg. Chem.* 2001; 627: 2100.
- [39] Halgren TA, Lipscomb WN. *Chem. Phys. Lett.* 1977; 49: 225.
- [40] Mulliken RS. *J. Chem. Phys.* 1955; 23: 1833.
- [41] Perdew JP, Wang Y. *Phys. Rev. B* 1992; 45: 13244.
- [42] Altarawneh M, Dlugogorski BZ, Kennedy EM, Mackie JC. *J. Phys. Chem. A* 2010; 114: 1098.
- [43] Altarawneh M, Kennedy EM, Dlugogorski BZ, Mackie JC. *J. Phys. Chem. A* 2008; 112: 6960.
- [44] Sun Q, Bu YX, Qin M. *J. Phys. Chem. A* 2003; 107: 1584.
- [45] Sun Q, Doerr M, Li Z, Smith SC, Thiel W. *Phys. Chem. Chem. Phys.* 2010; 12: 2450.
- [46] Sun Q, Li Z, Du A, Chen J, Zhu Z, Smith SC. *Fuel* 2012; 96: 291.
- [47] Sun Q, Li Z, Wang M, Du A, Smith SC. *Chem. Phys. Lett.* 2012; 550: 41.
- [48] Bader RFW. 1990. *Atoms in Molecules: A Quantum Theory*. New York, Oxford University Press
- [49] McElligo, Pe, Roberts RW. *J. Chem. Phys.* 1967; 46: 273.

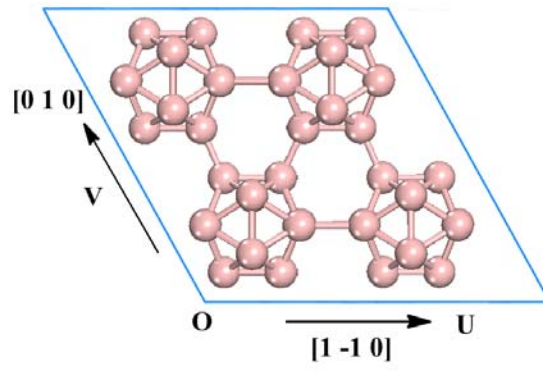


**Figure 1**

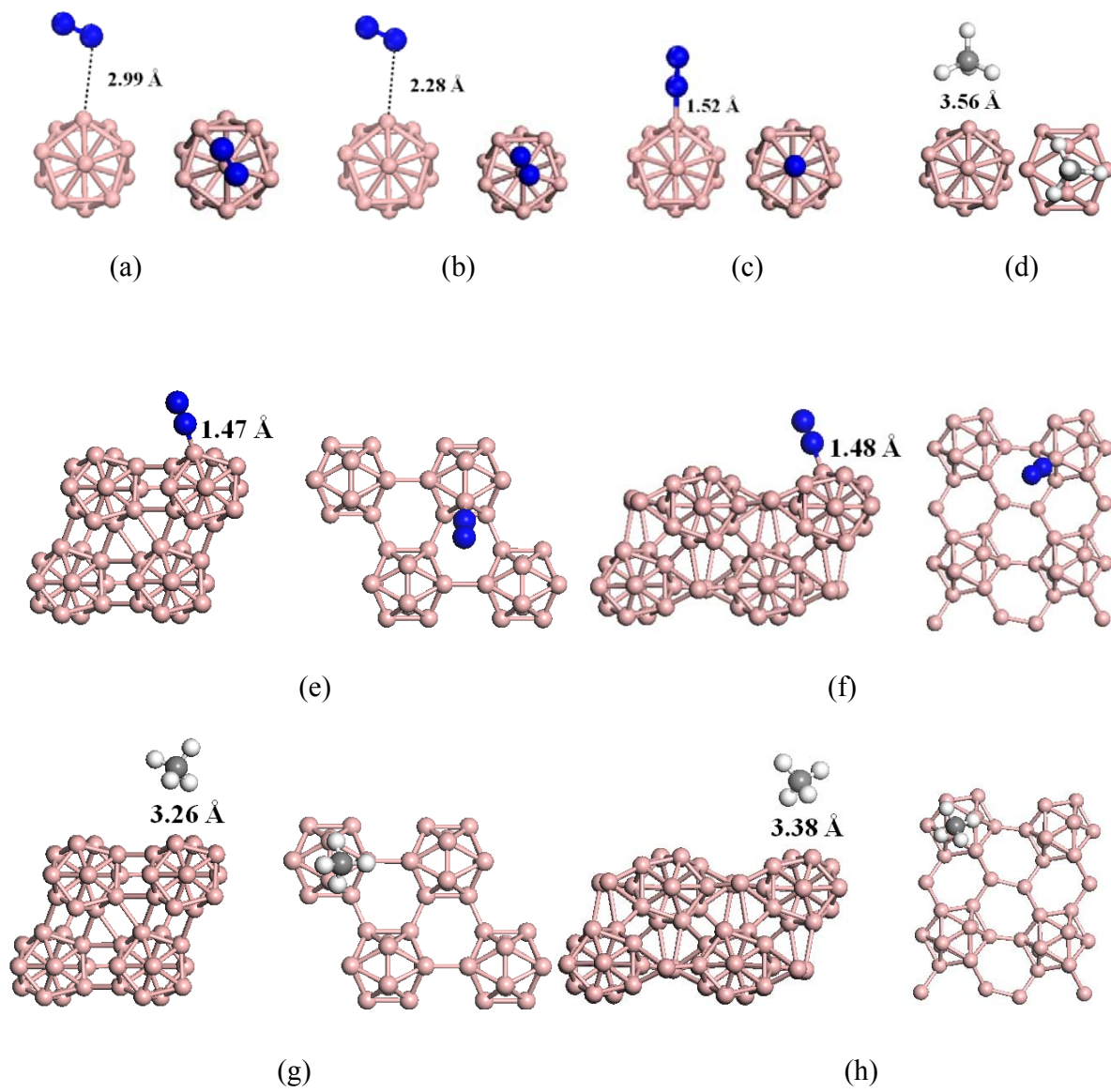


**Figure 2**

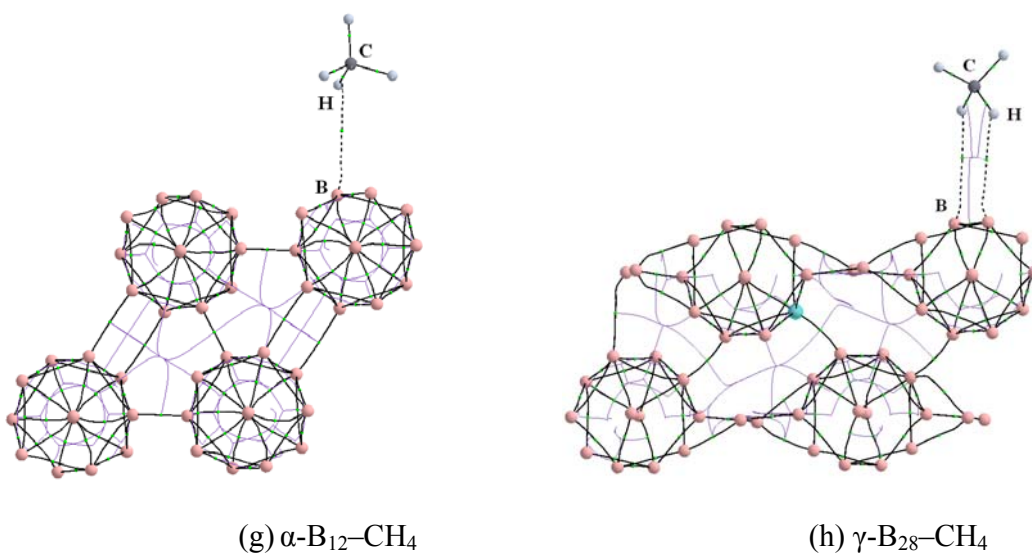
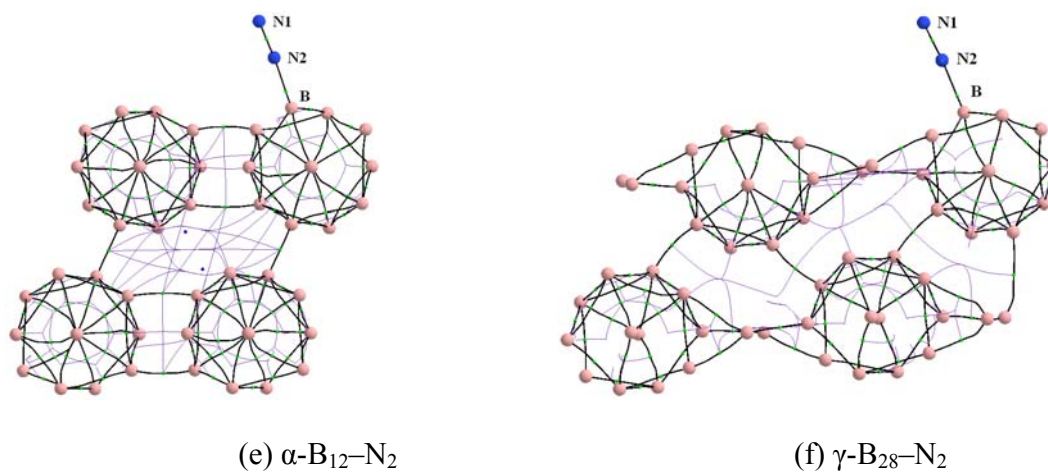
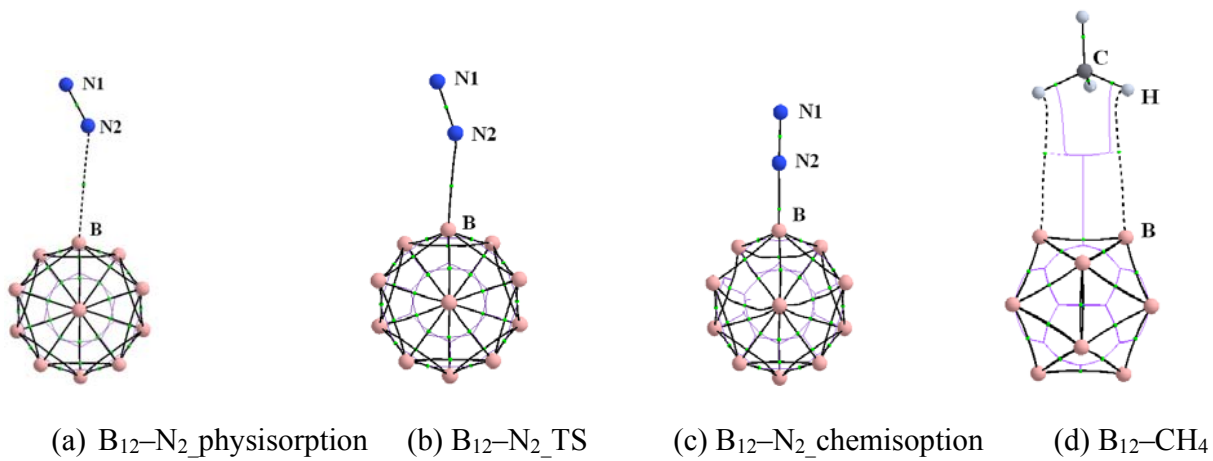


**Figure 3**

Table 1. Adsorption energy in eV, bond distance ( $r$ ) in Å and bond angle ( $\alpha$ ) in deg for  $N_2$  adsorption on  $B_{12}$  cluster,  $\alpha$ - $B_{12}$  and  $\gamma$ - $B_{28}$  surfaces.

Models	Physisorption	Transition state	Chemisorption
$B_{12}$ cluster	Adsorption energy	0.08	0.38
	$r(B...N)$	2.990	1.515
	$r(N-N)$	1.110	1.132
	$\alpha$ (B–N–N)	115.0	178.6
$\alpha$ - $B_{12}$	Adsorption energy		1.20
	$r(B...N)$		1.469
	$r(N-N)$		1.126
	$\alpha$ (B–N–N)		175.2
$\gamma$ - $B_{28}$	Adsorption energy		1.07
	$r(B...N)$		1.479
	$r(N-N)$		1.124
	$\alpha$ (B–N–N)		175.7

Table 2. Adsorption energy in eV, bond distance ( $r$ ) in Å and bond angle ( $\alpha$ ) in deg for  $CH_4$  adsorption on  $B_{12}$  cluster,  $\alpha$ - $B_{12}$  and  $\gamma$ - $B_{28}$  surfaces.

	$B_{12}$	$\alpha$ - $B_{12}$	$\gamma$ - $B_{28}$
Adsorption energy	0.08	0.17	0.14
$r(B...C)$	3.557	3.255	3.380
$r(B...H)$	2.833	2.807	2.676